

# Virtual Spacetime: An Environment for the Visualization of Curved Spacetimes via Geodesic Flows

Steve Bryson

RNR Technical Report RNR-92-009

March 1992

bryson@nas.nasa.gov

**(Note: some of the graphics described in this paper are missing. We regret the inconvenience.)**

## Abstract

We describe an implementation of a virtual environment for visualizing the geometry of curved spacetime by the display of interactive geodesics. This technique displays the paths of particles under the influence of gravity as described by the general theory of relativity, and is useful in the investigation of solutions to the field equations of that theory. A boom-mounted six degree of freedom head position sensitive stereo CRT system is used for display. A hand position sensitive glove controller is used to control the initial positions and directions of geodesics in spacetime. A multiprocessor graphics workstation is used for computation and rendering. We describe and illustrate with examples several techniques for visualizing the geometry of spacetime using geodesics. Though this work is described exclusively in the context of physical four-dimensional spacetimes, it extends to arbitrary geometries in arbitrary dimensions. While this work is intended for researchers, it is also useful for the teaching of general relativity.

## 1: Introduction

According to the theory of general relativity, the motion of objects under the influence of gravity can be understood in terms of objects moving along the straightest paths in a curved four-dimensional spacetime [1][2][3]. The curvature is determined by the distribution of the mass and energy in spacetime. Given the curvature, this paper is concerned with the visualization of that curvature by studying the straightest lines, or geodesics, in that spacetime. These geodesics correspond to the actual paths of particles under the influence of gravity. Geodesics can exhibit complex three-dimensional structure, and can vary widely depending on their initial locations and directions. Virtual environments provide a natural three-dimensional display and control capability for the investigation of geodesics. The use of paths for the visualization of geometry and the interactive display and control paradigms described in this paper are inspired by earlier work on the virtual windtunnel [4].

Geodesics in curved spacetime can be defined in a variety of equivalent ways. We shall treat geodesics as solutions of a set of ordinary second-order differential equations which will be introduced in section 2.3. The initial conditions for these equations are an initial position and direction of a geodesic. The solution to these equations are paths that are equivalently: 1) the shortest (or longest) path between any two points on the path, or 2) the path of a particle in spacetime that is not under any acceleration. The geometry of a spacetime completely determines the geodesics. We can use geodesics to study both the curvature of spacetime and the physical motion of objects in that spacetime. Thus the visualization of spacetime via display of geodesics provides both geometric

and physical insight.

This paper describes an implementation of an interactive virtual environment [4] which is dedicated to the exploration of curved spacetimes through the interactive display of geodesics (figure 1). The spacetimes considered are solutions to Einstein's equations, which specify the curvature of spacetime for a given distribution of matter and energy. The curved spacetime data provided can be closed form formulas or numerical data. Geodesics in spacetime are one-dimensional paths in four-dimensional space. The ability to rapidly move the geodesics around allows the researcher to get a sense of the overall curvature of spacetime. The interactive capability is provided by a VPL Dataglove, which measures the user's hand position, orientation and gesture. The three-dimensional structure of the geodesics is displayed via the Fake Space BOOM, a head-tracked wide field stereoscopic display system containing two monochromatic CRT monitors. The exploration capability requires the visualization software to compute and display the geodesics in response to the user inputs at a rate of about eight frames/second or better. To provide this performance, the geodesics are computed and rendered on a Silicon Graphics Iris 380GT/VGX workstation. Further details of this interface are discussed in section 4.

In section 1.1 we provide a brief survey of the role of visualization in general relativity. In section 2, the relevant mathematical framework is introduced. Section 3 describes the control and display of geodesics. The virtual environment hardware is introduced in section 4. Section 5 discusses the implementation of virtual spacetime, including visualization tools based on geodesics and their use in an example curved spacetime. Section 6 presents future work.

## 1.1 Visualization and General Relativity

Historically, visualization has played an important role in the development and presentation of general relativity. Many modern texts in general relativity (e. g. [1][3]) contain pictures which use visual arguments to motivate and argue significant technical points. This usefulness of visualization derives from the fact that general relativity is fundamentally a geometric theory. With the exception of Einstein's equations, which express the dependence of the curvature on the matter and energy distribution, the entire content of general relativity is to be found in the examination of curved space through the mathematics of differential geometry. Thus the visual display of the shapes of various aspects of spacetime geometry can provide real physical insight.

The difficulty of visualization in general relativity is that a curved spacetime is a four dimensional object. The difficulties of visually displaying the geometry of four-dimensional spaces are considerable. There are several methods in common use in general relativity to surmount these difficulties. They fall into two broad categories: embedding diagrams and physical simulations.

Embedding diagrams [1] are curved two-dimensional surfaces in flat three-dimensional space whose geometry corresponds with that of a two-dimensional slice through the curved four-dimensional spacetime. While embedding diagrams are a visually striking method of displaying curvature, they provide only indirect physical insight and only exist for simply curved spacetimes.

Physical simulations are typically based on the computation of geodesics. This is often done via direct computation of the paths in closed form [1][5]. This is a powerful method of studying the physical significance of a curved spacetime. Closed form computations are possible only in cases of simple curvatures. Numerical computation of geodesics can be done for general spacetimes, including the results of numerical spacetime calculations [6][7]. The technique discussed in this paper uses computational geodesics and provides a real-time

three-dimensional interface for both display and control of geodesics.

An important class of geodesics corresponds to light rays, called *lightlike* or *null* geodesics. These geodesics are usually displayed by replacing one space direction (usually the  $z$  axis) with the time direction. These geodesics are important because causal influences in spacetime travel at speeds slower than or equal to light. Displaying the paths of light rays give information about the causal structure of the spacetime. A *light cone* is the display of the initial directions of lightlike geodesics emanating from a point. In highly curved spacetimes, there can be causally disconnected regions of spacetime separated by an *event horizon*. Black holes are the most famous example of this phenomena. The mapping of event horizons in dynamic, numerical spacetimes is of great interest to physicists. The interactive visualization of lightlike geodesics described in this paper is well suited to this problem.

## 2: Spacetime, Geometry Data, and Geodesics

This section outlines the mathematics and concepts necessary to compute geodesics in spacetime given the geometry data for that spacetime. The necessary concepts will be given without motivation, proof, or complete context. Only information required to implement our visualization environment is given. For more detail, the reader should refer to the standard texts [1][2][3].

### 2.1 Spacetime and World Lines

Physics takes place in a four-dimensional space, called spacetime [8], which is the direct union of the three-dimensional space of our experience with time taken as a direction. From this point of view, objects which are bounded in space are, due to their persistence in time, extended objects in spacetime. Their extent in the time direction (in appropriate units) is much greater than their extent in the space direction. This gives the appearance of forming a line in spacetime oriented in the time direction called the object's *world line*. All objects in three-dimensional space form world lines in spacetime, so the study of the physics of objects in spacetime is the study of the behavior of the world lines of those objects. When these objects are not subject to any physical forces other than gravity, their world lines will be geodesics in curved spacetime.

Some simple examples will bring out important aspects of world lines. Consider a stationary object relative to some reference frame in three-dimensional space. In spacetime, that object is moving in the time direction. We can represent this motion in time by drawing a spacetime diagram, a two-dimensional diagram with the horizontal direction representing position in space and the vertical direction representing the position in time (figure 2). In this diagram, our motionless object has a world line that is vertical and parallel to the time axis.

An object moving from left to right will have a tilted world line. The slope of the moving object's world line will be  $1/(\text{speed of object})$ . The velocity of an object in three-dimensional space corresponds to a tilt of that object's world line in spacetime, so specifying a velocity in three-dimensional space is the same as specifying a direction in spacetime. We will use this fact to control the initial direction of geodesics in curved spacetime. An object under some varying acceleration will have a curved world line (figure 2).

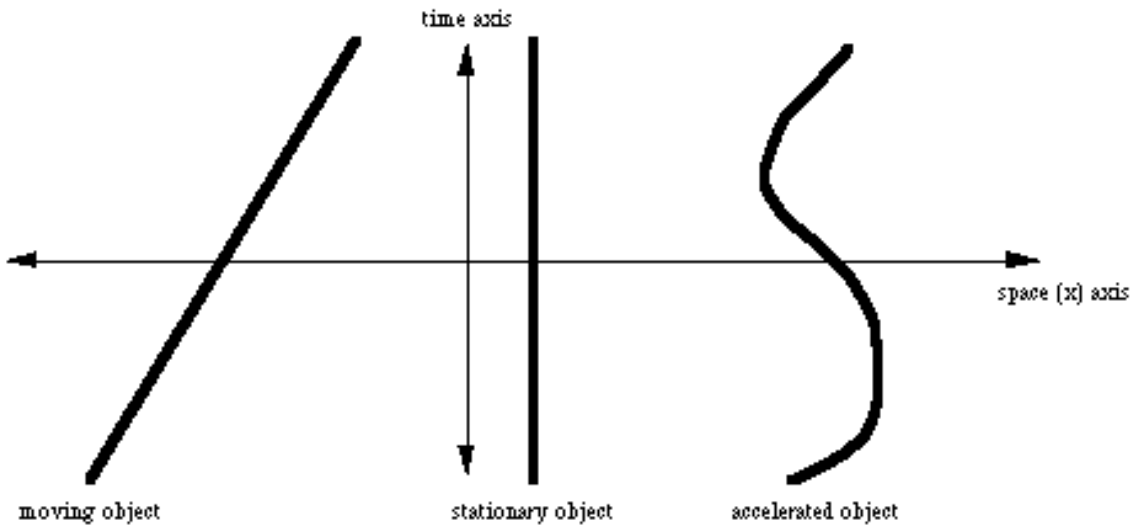


Figure 2. Example spacetime diagram showing world lines in a flat spacetime.

The spacetime diagram discussed above assumes a flat spacetime. If the spacetime is curved, the straight world lines would become curved geodesics. If these geodesics were observed without knowledge of the curvature of the spacetime, one would say that the objects corresponding to those curved world lines were accelerated by a force. In fact, they are not accelerated by a force but are following the curvature of spacetime. This is why gravity looks like a force when it is in fact due to the curvature of spacetime.

While space and time are directions in the geometric sense, the geometry in the time direction is different from that in the space directions. This is true for both flat and curved spacetime. For the moment, let us discuss the flat spacetime case. We can express the geometry of a space in terms of the formula for the distance between two points. In three-dimensional space, the distance between two points is given by the familiar Pythagorean theorem:

$$d^2 = (\Delta x)^2 + (\Delta y)^2 + (\Delta z)^2$$

where  $x$ ,  $y$ , and  $z$  are the usual Cartesian coordinates and  $d$  is the distance. In spacetime the distance formula is given by:

$$s^2 = c^2(\Delta t)^2 - (\Delta x)^2 - (\Delta y)^2 - (\Delta z)^2$$

where  $t$  is the time coordinate,  $s$  is the distance in spacetime and  $c$  is the speed of light. In this convention we have chosen the 'timelike' convention, so that  $s^2$  is positive for physical world lines which satisfy  $c^2(\Delta t)^2 > (\Delta x)^2 + (\Delta y)^2 + (\Delta z)^2$  for any two points on that world line (called a timelike world line). A *spacelike* world line satisfies the inequality  $c^2(\Delta t)^2 < (\Delta x)^2 + (\Delta y)^2 + (\Delta z)^2$  and corresponds to the path of a particle that moves faster than the speed of light. One could just as easily have chosen the 'spacelike' convention, reversing the signs in the distance formula. We shall adopt the timelike convention throughout this paper.

The spacetime distance formula has the remarkable property that  $s$  can have the value zero for physically separate points. A world line of a light ray has the property  $s = 0$  for any two points along that world line, and are called *lightlike* or *null* geodesics. Null geodesics play an important role in spacetime visualization.

## 2.2 Geometry Data: Metrics

The mathematical description of curved spacetime in general relativity is based on pseudo-Riemannian geometry, a part of differential geometry that describes the curvature of a space via distance relations between points of that space. For a general curved space of any dimension, these distance relations are expressed in a generalization of the Pythagorean theorem.

Let  $dx^{\mu}$  denotes an infinitesimal distance in the  $x^{\mu}$  direction in some coordinate system, where greek indices range from 0 to 3 with 0 labeling the time coordinate. The distance formula in spacetime is given by:

$$ds^2 = \sum_{\mu, \nu=0}^3 g_{\mu\nu}(x) dx^{\mu} dx^{\nu}$$

where each  $g_{\mu\nu}(x)$  is an entry in a 4x4 matrix  $g(x)$  of functions of a point  $x$  in spacetime called the *metric*. In the case of flat spacetime described in section 2.1 above, the metric is given by

$$g(x) = \text{Bbc}((\text{Aalhs5co4}(c^2, 0, 0, 0, 0, -1, 0, 0, 0, 0, -1, 0, 0, 0, 0, -1))$$

In a general curved spacetime, any of the entries in the metric may be a non-constant function. On the other hand, the example of the distance formula in flat two dimensional space in polar coordinates,  $d^2 = (\Delta r)^2 + r^2 (\Delta \theta)^2$  shows that non-constant functions in the metric do not imply curvature. The Riemann curvature tensor is a function of the first and second derivatives of the metric which vanishes if and only if the space described by that metric is flat. This curvature tensor appears linearly as part of Einstein's field equations of general relativity, so Einstein's equations are second-order non-linear partial differential equations for the metric. Solutions to these equations for a particular distribution of matter are physical metrics that describe physical spacetime.

Metrics are computed in particular coordinate systems suited to different physical aspects of the spacetime. The same physical spacetime is often described in different coordinates, implying different formulas for the metric. Since the metric is used to compute the geodesics of a spacetime, we will take as the basic geometry data for a spacetime a coordinate system and metric in those coordinates. These data can be in the form of exact closed form formulas, or as data on a computational grid.

## 2.3 Computing Geodesics

Given a metric  $g(x)$ , the geodesic starting at the point  $x^{\mu} = (x^0, x^1, x^2, x^3)$  with initial spacetime direction  $dx/ds = (dx^0/ds, dx^1/ds, dx^2/ds, dx^3/ds)$ , where  $s$  is a parameter often taken to be arc length, may be obtained by iteratively solving the geodesic equations [1][2][3]:

$$F(d^2 x^{\mu}, ds^2) = \sum_{\nu, \lambda=0}^3 \Gamma^{\mu}_{\nu\lambda}(x) F(dx^{\nu}, ds) F(dx^{\lambda}, ds)$$

The  $\Gamma^{\mu}_{\nu\lambda}(x)$  are functions of  $g(x)$ , and are given by

$$\Gamma^{\mu}_{\nu\lambda}(x) = \sum_{\alpha=0}^3 F(1, 2) g^{\mu\alpha}(x) \text{Bbc}((F(dg^{\alpha}_{\nu\lambda}))(i>x),$$

$$dx[[[\lambda]]] + F(dg[[\alpha]][[\lambda]](x), dx[[[\nu]]] - F(dg[[\nu]][[\lambda]](x), dx[[[\alpha]]]))$$

These  $[[\Gamma]]_{[u][\nu]][[\lambda]](x)$  are called connection coefficients or Christoffel symbols, and  $g_{[u][\nu]}(x)$  are the entries of the matrix  $g_{[-1]}(x)$ . Connection coefficients measure how tangent vectors in curved spacetime are turned by the curvature as they are translated in spacetime. Thus the geodesic equations are the equations for the "least turning" path in a curved spacetime, or equivalently they are the equation "acceleration relative to curved spacetime = 0". The connection coefficients are symmetric in two indices and so have 40 independent components. The connection coefficients can be numerically computed from metric data, but this induces numerical error and is time consuming. We have found it advantageous to include the connection coefficients as part of the geometry data. When the metric is available as exact formulas, the formulas for the connection coefficients are derived and included in the geometry data. For computational spacetimes, the metric and connection coefficients are directly available as data on a computational grid.

A numerical solution to the geodesic equations is obtained by selecting a  $[[\Delta]]s$  and integrating once to obtain, for each value of  $u$ , a new  $dx_{[u]}/ds$ , which is again integrated to find a new  $x_{[u]}$ . This process is repeated, producing a path  $x(s) = (x_{[0]}(s), x_{[1]}(s), x_{[2]}(s), x_{[3]}(s))$ , which can then be displayed for visualization. When  $[[\Delta]]s$  is sufficiently small, Euler integration is sufficient. At the  $n$ th step,  $s = n[[\Delta]]s$ , so using Euler integration the solution to the geodesic equations at the  $n$ th step is given by

$$F(dx_{[u]}(n[[\Delta]]s), ds) = [[\Delta]]s \text{Isu}(L([[\nu]], [[\lambda]])=0), 3, \text{Bbc}([[\Gamma]]_{[u][\nu]][[\lambda]](x((n-1)[[\Delta]]i>s))) F(dx[[[\nu]]]((n-1)[[\Delta]]s), ds) F(dx[[[\lambda]]]((n-1)[[\Delta]]s), ds)),$$

$$x_{[u]}(n[[\Delta]]s) = [[\Delta]]s F(dx_{[u]}(n[[\Delta]]s), ds).$$

It is not always possible to choose a small  $[[\Delta]]s$  however, since one desires a sufficiently long path to display the geometry of spacetime over long distances. With a small  $[[\Delta]]s$ , many iterations would be required to produce a path of sufficient length. We also require, however, that the geodesics be computed and displayed sufficiently quickly that one can move the geodesics around in real time, and display them from a moving point of view. This puts a constraint on the number of points that can be computed for a path. Thus larger values of  $[[\Delta]]s$  can become necessary, in which case a more accurate numerical integration method than Euler integration may be required. We have found the Adams-Bashforth predictor-corrector integration [9] fast enough to be useful.

### 3: Control and Display of Geodesics

#### 3.1 Mapping User Inputs to Geodesic Initial Conditions

Giving the user real-time control of geodesics amounts to giving the user control over the initial position  $x_{[j]} = (x_{[0]}, x_{[1]}, x_{[2]}, x_{[3]})$  and the initial direction vector  $dx/ds = (dx_{[0]}/ds, dx_{[1]}/ds, dx_{[2]}/ds, dx_{[3]}/ds)$ . As pointed out in section 2.1, the initial direction in four-dimensional spacetime can be thought of as a velocity vector in three-dimensional space. Using the VPL Dataglove, which provides the position and orientation of the user's hand, the user's hand position can be used to control the initial three-dimensional position of the geodesic. The initial time can be chosen as the current timestep in the case of dynamic spacetimes. The orientation of the user's hand in combination with a preset velocity magnitude can be used to control the initial direction vector. The precise mapping from the velocity vector to the initial spacetime direction will be described in sections 3.2.

We control the preset velocity magnitude "off-line" using mouse controls. In this design the user is interacting with the geodesic path of a particle with a fixed velocity and interactively controlled initial direction. This choice is motivated by ease of implementation and the direct physical intuition it provides. Other choices of control would be interesting to explore. These could include using the degree of bend of a finger or some other interactive control.

Typically, the graphics coordinate system will not be the same as the coordinate system in the geometry data. The initial position and orientation vector input by the user must be converted to the coordinate system in the geometry data. The form of the coordinate part of the geometry data should include the transformation to some standard coordinate system such as euclidean coordinates and the jacobian of that coordinate transformation for the conversion of the direction vector.

### 3.2 Computation of Initial Spacetime Direction

When possible, we will be parametrizing our geodesics by arc length in spacetime. This is not possible for null geodesics, however, as they have spacetime arc length = 0. When converting the velocity vector to an initial spacetime direction vector, the timelike geodesics and null geodesics must be handled differently. We do not consider spacelike geodesics, which are currently believed to be unphysical. The kind of geodesic being generated is determined by the length of the initial velocity vector, which is computed by using the spacetime metric.

In this section the indices  $i$  and  $j$  refer to the three-dimensional space coordinates in the four-dimensional spacetime, and range from 1 to 3 and we denote the time coordinate by  $t$ . From the definition of the metric in section 2.2,

$$ds^2 = g_{00}(\mathbf{x}) dt^2 + 2 \sum_{i=1}^3 g_{i0}(\mathbf{x}) dx^i dt + \sum_{i,j=1}^3 g_{ij}(\mathbf{x}) dx^i dx^j$$

dividing by  $dt^2$ ,

$$Bbc((F(ds,dt))^2) = g_{00}(\mathbf{x}) + 2 \sum_{i=1}^3 g_{i0}(\mathbf{x}) v^i + \sum_{i,j=1}^3 g_{ij}(\mathbf{x}) v^i v^j, \quad (1)$$

where  $\mathbf{v} = dx/dt$  is just the three-space velocity ( $dx^i/dt = v^i$ ). In the case of timelike lines, this will be greater than zero and we can solve for  $F(dt,ds)$  :

$$F(dt,ds) = Bbc((g_{00}(\mathbf{x}) + 2 \sum_{i=1}^3 g_{i0}(\mathbf{x}) v^i + \sum_{i,j=1}^3 g_{ij}(\mathbf{x}) v^i v^j))^{1/2} = F(1,2). \quad (2)$$

This gives one component of the initial spacetime direction. The other components are found via the chain rule:

$$F(dx^i, ds) = F(dx^i, dt) F(dt, ds) = v^i F(dt, ds)..$$

For null lines, the above expression for  $Bbc((F(ds,dt))^2)$  vanishes and we cannot simply solve for  $F(dt,ds)$ . In this case the magnitude of the velocity is set to the speed of light and we can use an arbitrary parameterization of the geodesic. This allows us to set the  $F(dt,ds)$  component of the initial spacetime direction to an arbitrary value. Note that because the speed of light is, by definition, the velocity for which the spacetime distance vanishes,

which is in turn dependent on the local geometry through the metric, the value of the speed of light in a fixed coordinate system will vary from point to point in space. Given a spacetime velocity vector, the magnitude of that vector may be greater than the speed of light in some regions of spacetime. We shall always consider such cases to be initial directions for null geodesics. Thus given a velocity vector  $\mathbf{v}$  at some position  $\mathbf{x}$  in space, when the magnitude of  $\mathbf{v}$  is greater than the speed of light at  $\mathbf{x}$ , we must scale  $\mathbf{v}$  so that its magnitude is exactly the speed of light at  $\mathbf{x}$ . Let  $a$  denote this scale factor, so  $\mathbf{v} \rightarrow a\mathbf{v}$ . Substituting  $a\mathbf{v}$  into the expression for  $B_{bc}((F(ds,dt))$  [2] gives:

$$0 = g_{00}(\mathbf{x}) + 2a \text{Isu}(L(i=1),3, g_{i0}(\mathbf{x}) v^{[i]}] + a^2 \text{Isu}(L(i,j=1),3, g_{ij}(\mathbf{x}) v^{[i]} v^{[j]}].$$

This is a quadratic equation for  $a$ . Setting  $A = \text{Isu}(L(i,j=1),3, g_{ij}(\mathbf{x}) v^{[i]} v^{[j]})$  and  $B = 2 \text{Isu}(L(i=1),3, g_{i0}(\mathbf{x}) v^{[i]})$ , we find

$$a = \text{Blc}\{(A \pm \sqrt{A^2 - 4g_{00}(\mathbf{x}) B}) / (2A)\} \quad A \neq 0, \quad F(-g_{00}(\mathbf{x}), B) A = 0$$

The three space components of the initial spacetime direction are found in the same way as in the timelike case:

$$F(dx^{[i]}, ds) = F(dx^{[i]}, dt) F(dt, ds) = av^{[i]} F(dt, ds)..$$

### 3.2 The Display of Geodesics

The geodesics that result from the calculations described above are paths  $\mathbf{x}(s) = (x^{[0]}(s), x^{[1]}(s), x^{[2]}(s), x^{[3]}(s))$  in four dimensions. This path must be converted into the appropriate coordinates for display using the coordinate part of the geometry data. Since each point on the path has four components and our virtual environment renders these paths in a virtual three-dimensional space, there is some freedom as to how these paths are mapped to the display. There are standard possibilities.

The first possibility is to map the spatial part of the paths  $(x^{[1]}(s), x^{[2]}(s), x^{[3]}(s))$  to the three dimensional graphics space directly. This choice will be called a *spatial display*. The paths in this display are the paths in space followed by pointlike objects of infinitesimal mass under the influence of the gravity generated by the curvature of that spacetime.

The second possibility is to map the coordinates  $\mathbf{x}(s) = (x^{[0]}(s), x^{[1]}(s), x^{[2]}(s), x^{[3]}(s))$  to the three-dimensional point  $(x^{[1]}(s), x^{[2]}(s), x^{[0]}(s))$  replacing the third spatial coordinate by the time coordinate, along with any necessary coordinate transformations. This choice will be called a *spacetime display*. The paths in this display are the world lines of pointlike objects as in the previous paragraph.

The exploration of other display options are of great interest. It would be interesting to explore the freedom that a virtual environment provides by developing mixed spatial and spacetime displays.

## 4: The Virtual Environment Interface

The virtual environment interface provides a natural three-dimensional environment for both display and control of geodesics. This interface allows intuitive exploration of rich, complex geometries. It is very similar to the interface used in the virtual windtunnel [4]. The basic components of the environment are: a high-performance

graphics workstation for computation and rendering, a BOOM for display, and a VPL Dataglove for control (fig. 3).

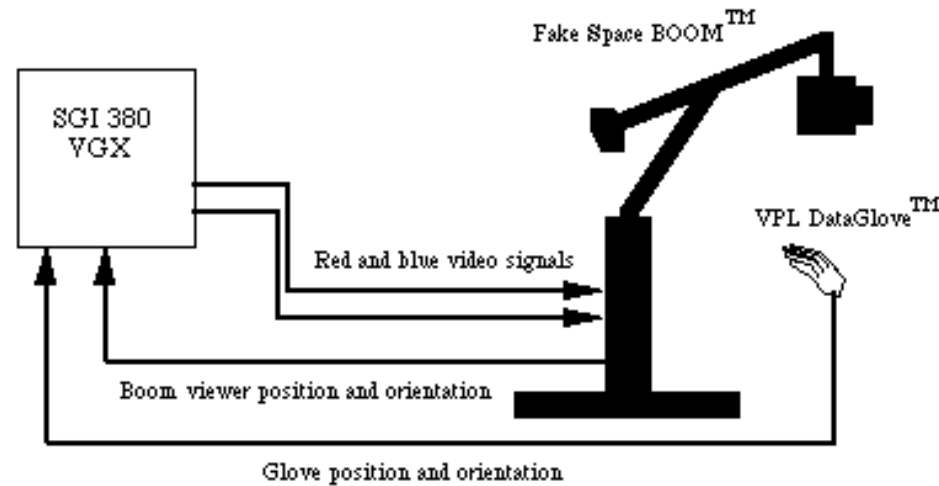


Fig 3: The hardware configuration of the virtual windtunnel system.

The display for our virtual environment is the BOOM, manufactured by Fake Space Labs of Menlo Park CA., and fashioned after the prototype developed earlier by Sterling Software, Inc. at the VIEW lab at NASA Ames Research Center [11] (figure 4).

The boom is a CRT based alternative to the popular head-mounted LCD display systems that were pioneered at the VIEW lab [12] and are now widely used. The boom provides much better brightness, contrast, and resolution than standard liquid crystal displays. Two monochromatic RS170 CRTs are provided, one for each eye, so that the computer generated scene may be viewed in stereo. The CRTs are viewed through wide field optics provided by LEEP Optics, so the computer generated image fills the user's field of view. The weight of the CRTs are borne by a counterweighted yoke assembly with six joints, which allow easy movement of the head with six degrees of freedom within a limited range. Optical encoders on the joints of the yoke assembly are continuously read by the host computer providing the six angles of the joints of the yoke. These angles are converted into a 4x4 matrix containing the position and orientation of the BOOM head by six successive translations and rotations. By inverting this position and orientation matrix and concatenating it with the graphics transformation matrix stack, the computer generated scene is rendered from the user's point of view. As the user moves, that point of view changes in real-time, providing a strong illusion that the user is viewing an actual three-dimensional environment.

For user control in our virtual environment the user's hand position, orientation, and finger joint angles are sensed using a VPL dataglove(TM) model II, which incorporates a Polhemus 3Space(TM) tracker. The Polhemus tracker gives the absolute position and orientation of the glove relative to a source by sensing multiplexed orthogonal electromagnetic fields. The degree of bend of knuckle and middle joints of the fingers and thumb of the user's hand are measured by the VPL Dataglove(TM) model II using specially treated optical fibers. These finger joint angles are interpreted as gestures.

The computation and rendering for our virtual environment is provided by a Silicon Graphics Iris 380 VGX system. This is a multiprocessor system with eight 33 MHz RISC processors (MIPS R3000 CPUs with R3010 floating point chips). The performance of the machine is rated at approximately 200 MIPS and 37 linpack megaflops. Our system has 256 MBytes of memory. The rated graphics performance of our system is about

800,000 small triangles per second.

Stereo display on the boom is handled by rendering the left eye image using only shades of pure red (of which 256 are available) and the right eye image using only shades of pure blue. The 1024x1280 pixel RGB video output of the VGX is converted into RS170 component video in real time using a scan converter. The red component is fed into the left eye of the boom, and the blue component into the right eye. The sync is fed to both eyes. Since the boom CRTs are monochrome, we see correctly matched stereo images.

## 5: The Implementation of Virtual Spacetime

The implementation of the concepts described in section 3 with the interface described in section 4 will be discussed using a simple example spacetime, that of a non-rotating perfectly spherical mass of infinitesimal radius. The solution of Einstein's equations in this case is known in terms of closed functions and is known as the Schwarzschild solution. We will explicitly give the geometry data and discuss various tools and display options for visualization.

### 5.1 The Schwarzschild Solution

The Schwarzschild solution [1][2][3] is a solution to Einstein's equations corresponding to the exterior of a perfectly spherical, non-rotating body of mass  $m$ . This solution gives a good description of the spacetime around a planet or star and geodesics correspond to the paths of objects under the mass's gravitational influence. We shall choose time and mass units, called natural units, so that the speed of light  $c$  and Newton's gravitational constant  $G$  both have the values  $c = G = 1$ . In these units both time and mass have units of length. We shall work in Schwarzschild coordinates  $(t, r, [\theta], [\phi])$ , which correspond to spherical coordinates at infinity and have a simple physical meaning. These coordinates are related to Cartesian coordinates  $(t, x, y, z)$  by

$$x = r \sin[\theta] \cos[\phi]$$

$$y = r \sin[\theta] \sin[\phi],$$

$$z = r \cos[\theta].$$

$$t = t$$

In these coordinates, the metric is

$$g(t, r, [\theta], [\phi]) = \text{Bbc}((A \text{alhs} 5 \text{co} 4(1 - F(2m, r)), 0, 0, 0, 0, -\text{Bbc}((1 - F(2m, r))^{-1}), 0, 0, 0, 0, -r^2, 0, 0, 0, 0, -r^2 \sin^2[\theta])).$$

The non-vanishing connection coefficients are:

$$[\Gamma]_{[t]rt} = [\Gamma]_{[t]tr} = F(m, r(r-2m))$$

$$[\Gamma]_{[r]rr} = -F(m, r(r-2m)), [\Gamma]_{[r][\theta][\theta]} = -(r-2m), [\Gamma]_{[r][\phi][\phi]} = -\sin^2[\theta](r-2m), [\Gamma]_{[r]tt} = F(m, r^2) \text{Bbc}((1 - F(2m, r)),$$

$$[[\Gamma]][[\theta]][[r]] = [[\Gamma]][[\theta]]r [[\theta]] = F(1,r) , [[\Gamma]][[\theta]][[\phi]][[\phi]] = -\sin[[\theta]]\cos[[\theta]]$$

$$[[\Gamma]][[\phi]][[r]] = [[\Gamma]][[\phi]]r [[\phi]] = F(1,r) , [[\Gamma]][[\phi]][[\phi]][[\theta]] = [[\Gamma]][[\phi]][[\theta]][[\phi]] = \cot[[\theta]]$$

It is apparent that there are two singularities in this metric, at  $r=0$  and  $r=2m$ . The singularity at  $r=0$  is a true singularity of the geometry in the sense that the curvature diverges there. The singularity at  $r=2m$  is the famous Schwarzschild radius and is an artefact of the coordinates which does not occur in other coordinate systems. This singularity is associated with an event horizon, however, since the region  $r<2m$  cannot send causal influences to the region  $r>2m$ . This is called a black hole, as anything that falls into the  $r<2m$  region can never come out again.

Using single geodesics, various features of the Schwarzschild solution may be discovered with the system described in this paper. Geodesics with initial direction perpendicular to the radius vector describe orbits of the spacetime. When these orbits are not circular, they show a characteristic rosette pattern that corresponds to the phenomena of precession of perihelia in planetary orbits around the sun [1][2] (figure 5). Null geodesics, which correspond to the paths of light rays, are seen to be bent and exhibit circular orbits when their initial directions are perpendicular to the radius vector at  $r=3m$  [1][2] (figure 5). In the spacetime display format, a geodesic with zero initial velocity magnitude, which corresponds to a freely falling object, is observed to asymptotically approach the Schwarzschild radius (figure 5). This shows the interesting phenomenon of an object taking forever to fall into a black hole when viewed from coordinates defined far away, despite the object falling into the black hole in a (short) finite time in its local coordinates [1][2]. Using geometry data for the Schwarzschild spacetime with another choice of coordinates called Eddington-Finkelstein coordinates [1][3], the geodesic of a freely falling object is seen to fall all the way to  $r = 0$  (figure 5).

The spacetime for a rotating body, called the Kerr solution [3], has also been implemented, and the geodesics corresponding to free-falling objects show a distinct falling 'pull' in the direction of the massive body's rotation (figure 5). This is known as the dragging of inertial frames [1][2][3].

## 5.2 Visualization tools

Visualization tools in virtual spacetime are single geodesics or groups of geodesics analogous to rakes in the visualization of simulated fluid flow [4]. The number of geodesics in a tool are constrained by performance requirements. We currently use at most eight geodesics in a tool distributed across the eight processors in the workstation. The position and orientation of the tools are manipulated with the VPL Dataglove. Tools that have been implemented besides single geodesics are sprays, rakes and tubes.

*Sprays* are groups of geodesics all of which have the same initial positions and velocity magnitudes but different initial directions (figure 6). Currently these directions all lay in the same plane which is oriented via the Dataglove. Sprays are useful for exploring the general geometry of a curved spacetime.

*Rakes* are lines of initial positions of geodesics all of which have the same initial velocity vectors. The geodesics are initially parallel and diverge or converge due to the curvature of spacetime (figure 6). This divergence and convergence correspond to tidal forces and are a direct visualization of the components of the Riemann curvature

tensor [1].

*Tubes* are analogous to rakes, with the initial positions distributed in a circle perpendicular to the initial velocities (figure 6). This allow the twisting tidal forces to be observed, along with other components of the curvature tensor.

A *lightsphere* is a set of short null geodesics with the same initial position whose initial directions are equidistributed over a sphere (figure 7). Lightspheres are useful for the detection of places of large curvature. By using very short geodesics, a full sphere in three-dimensional space may be displayed.

A *lightcone* is a spacetime display of the initial spacetime directions of a spray of null geodesics (figure 7). Lightcones are a standard visualization technique in general relativity, and are useful for probing the local causal structure of spacetime [1][2][3].

### 5.3 Performance

The real-time computation of geodesics requires fairly high computational power. The system described in this paper is capable of controlling, computing and displaying one to eight geodesics with lengths of about 300 points at about eight frames/second. This is sufficient for many purposes. A less expensive system capable of this performance with single geodesics is the Iris Indigo, which has a single MIPS R3000 processor. The computation of geodesics has also been implemented for a three-dimensional spacetime (time plus two space dimensions) on a Macintosh IICI, which takes less than two seconds to compute a geodesic with 200 points. While this is not sufficient for virtual environment interaction, it is sufficient for pedagogical purposes.

### 5: Further Work

The system described in this paper has demonstrated the feasibility of real-time interactive virtual environment techniques for the visualization of curved spacetimes using geodesics. Currently the system has been implemented only for spacetimes whose geometry data are available in closed form formulas and for spacetimes whose data are on simple static computational grids.

There are interesting spacetimes whose metrics are available as exact formulas. Incorporation into virtual spacetime should be straightforward. Examples include the classical Godel solution [3], Bianchi type IX cosmological solutions [12], and a metric describing collapsing dust or photons [13].

A more difficult problem is including the results of computational spacetime simulations such as those describing colliding black holes, collapsing stars, and gravitational waves [14]. There has been considerable interest expressed by the computational spacetime group at the National Center for Supercomputing Applications (NCSA) in Urbana, Illinois in using virtual spacetime to view the results of their computations. We are currently developing a collaboration for this purpose with Ed Seidel and Larry Smarr. Problems addressed by this collaboration include: the meaning of the coordinates used for the numerical simulation and how these coordinates should be mapped into the virtual space, developing an interpolation scheme to compute geometry data from the computational grid that is fast enough to allow real-time computation of geodesics; and managing the very large amounts of data that are the products of these unsteady spacetime computations. The data and speed problems are similar to those that arise in the virtual windtunnel [4]. Distributing the computation to a supercomputer over a high-speed network [15] may be necessary.

## 5: Acknowledgements

The author would like to thank Larry Smarr of NCSA for initial encouragement and dramatic enthusiasm in response to early versions of this system. The author's esteemed colleague Creon Levit deserves equal credit for helping to discover what virtual environments are good for and for many useful conversations. Thanks also to Ed Seidel for many useful discussions. Finally, thanks to Dan Asimov, Mike Gerald-Yamasaki, Al Globus, Tom Lasinski, Jeff Hultquist, and Creon Levit for comments on early versions of this paper.

- [1] C. W. Misner, K. Thorne, J. A. Wheeler, *Gravitation*, W. H. Freeman and Co., San Francisco, 1973
- [2] R. Wald, *General Relativity*, University of Chicago Press, Chicago, 1984
- [3] S. Hawking and G. F. R. Ellis, *The Large Scale Structure of Spacetime*, Cambridge University Press, Cambridge, England, 1973
- [4] S. Bryson and C. Levit, "The Virtual Windtunnel: An Environment for the Exploration of Three-Dimensional Unsteady Fluid Flows", *Proceedings of IEEE Visualization '91*, San Diego, Ca. 1991, to appear in *Computer Graphics and Applications* July 1992
- [5] S. Chandrasekhar, *The Mathematical Theory of Black Holes*, Clarendon Press, Oxford, 1983
- [6] S. L. Shapiro and S. A. Teukolsky, "Relativistic Stellar Dynamics on the Computer", *Dynamical Spacetimes and Numerical Relativity*, J. M Centrella, Ed., Cambridge University Press, Cambridge, England, 1986
- [7] D. H. Bernstein, D. W. Hobill, and L. L. Smarr, "Black Hole Spacetimes: Testing Numerical Relativity", *Frontiers in Numerical Relativity*, C. R. Evans, L. S. Finn, and D. W. Hobill, Ed., Cambridge University Press, Cambridge, England, 1989
- [8] E. F. Taylor and J. A. Wheeler, *Spacetime Physics*, W. H. Freeman and Co., New York, 1966
- [9] R. Beckett and J. Hurt, *Numerical Calculations and Algorithms*, McGraw-Hill, New York, 1967
- [10] I.E. McDowall, M. Bolas, S. Pieper, S.S. Fisher and J. Humphries, "Implementation and Integration of a Counterbalanced CRT-Based Stereoscopic Display for Interactive Viewpoint Control in Virtual Environment Application", in *Proc. SPIE Conf. on Stereoscopic Displays and Applications*, J. Merrit and Scott Fisher, eds. (1990).
- [11] Fisher, S. et. al., Virtual Environment Interface Workstations, *Proceedings of the Human Factors Society 32nd Annual Meeting*, Anaheim, Ca. 1988
- [12] M. Ryan, *Hamiltonian Cosmology*, Springer-Verlag, Berlin, 1972
- [13] J. P. S. Lemos, "Naked Singularities: Gravitationally Collapsing Configurations of Dust or Radiation in Spherical Symmetry, a Unified Treatment", *Physical Review Letters*, Vol. 68 No. 10, 9 March 1992

[14] C. R. Evans, L. S. Finn, and D. W. Hobill, Ed., *Frontiers in Numerical Relativity*, Cambridge University Press, Cambridge, England, 1989

[15] S. Bryson and M. Gerald-Yamasaki, "The Distributed Virtual Windtunnel", to appear (submitted to Supercomputing '92).

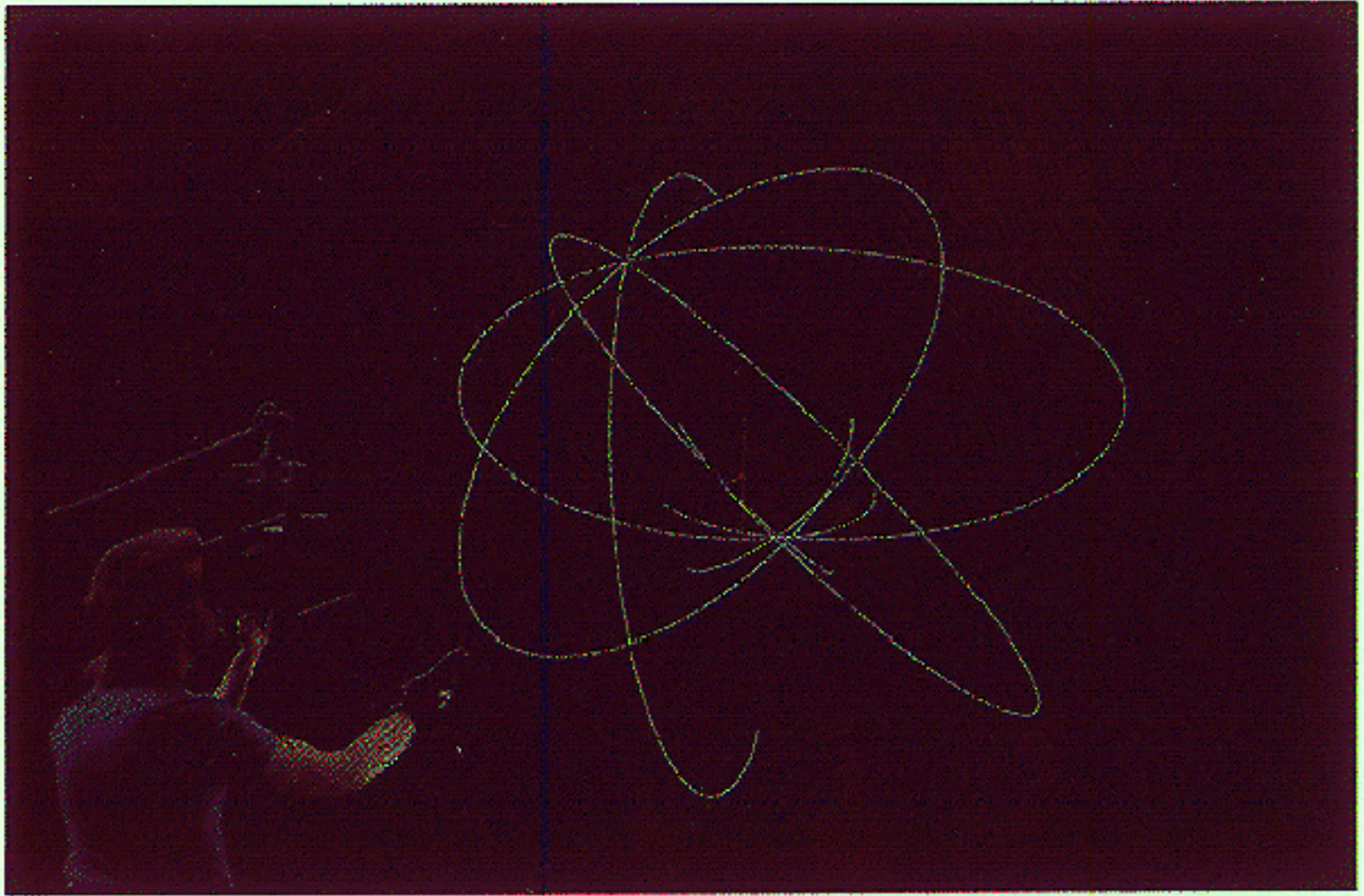


**Figure 1: The virtual spacetime system in use, showing the manipulation and observation of a spray of geodesics.**

Figure 1: An illustration of virtual spacetime in use. The user is manipulating a spray of geodesics in a curved spacetime with an instrumented glove while observing the results in a head-tracked, wide field of view stereo display.



Figure 4: The virtual interface hardware, showing the Fake Space Labs BOOM and the VPL Dataglove Model II.

Figure 5: Visualizing the spacetime around a spherical object of mass  $m$ , such as a star. The center of the star is

indicated by the yellow cross.

Top left: Geodesics forming almost circular orbits. The orbits do not close, but form a rosette pattern. This is called the precession of perihelia.

Top center: Orbits of light rays, including the circular orbit at  $r = F(3Gm, c^2)$ .

Top right: The orbits of light rays in a spacetime display where the vertical direction represents time.

Bottom left: Spacetime display of a particle falling from rest in Schwarzschild coordinates. The geodesic asymptotically approaches the distance  $r = F(2Gm, c^2)$  in these coordinates.

Bottom center: Spacetime display of the same particle in the same spacetime in Eddington-Finkelstein coordinates. In these coordinates the particle falls to  $r = 0$ .

Bottom right: Spatial view of the geodesic of an object falling from rest in the spacetime around a counter-clockwise rotating star (Kerr spacetime). The curvature due to the rotation bends the geodesic to the right.

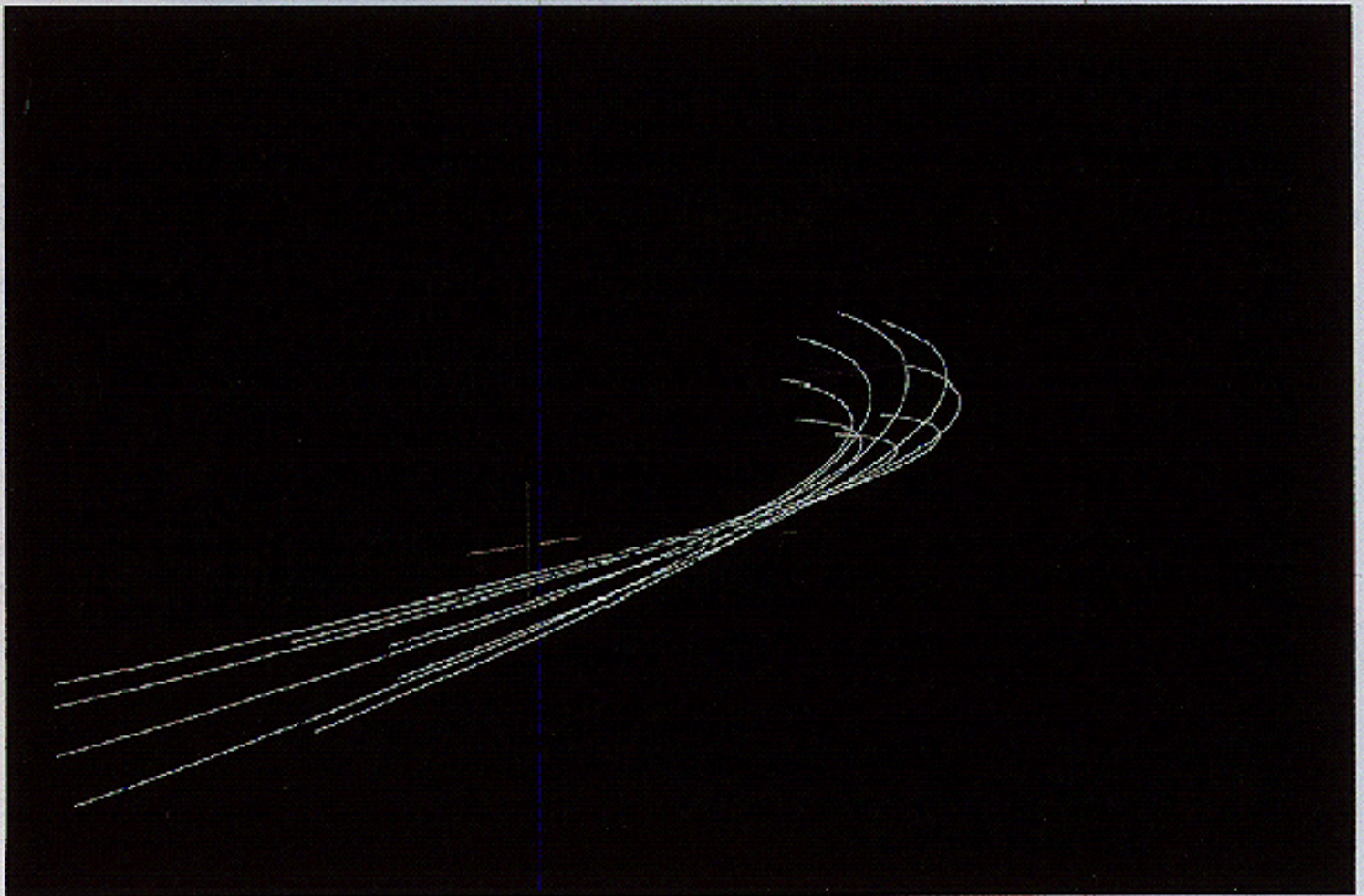


**Figure 4: A tube of geodesics.**

Spatial display of a tube of timelike geodesics. Note the focussing effect along the vertical direction.

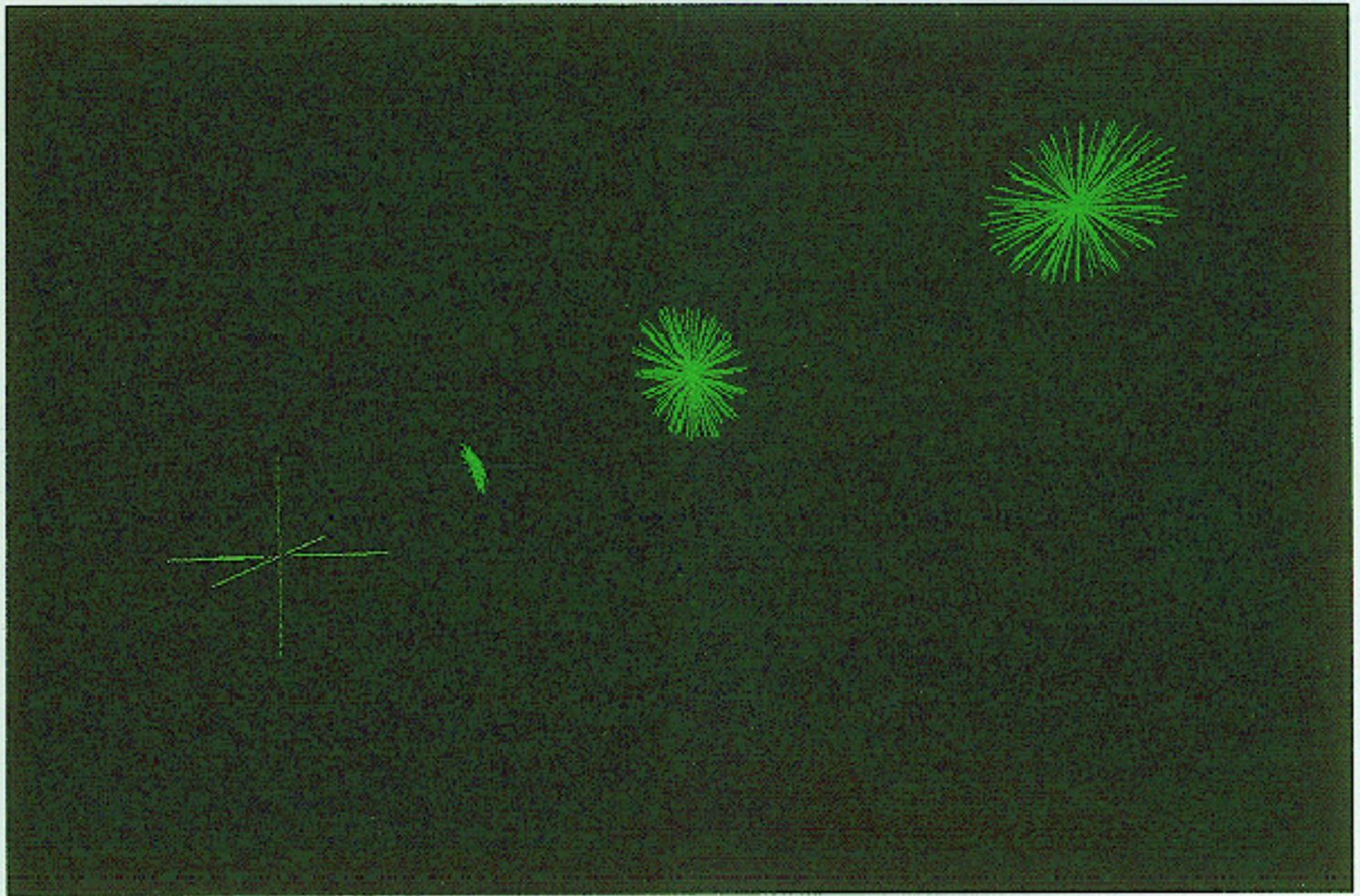


Figure 5: Lightspheres.

Spatial display of lightspheres at varying distances from the center of the object. Far from the center (right), the lightsphere is approximately spherical. Near the center of the object (left) the shape of the lightsphere is severely distorted.

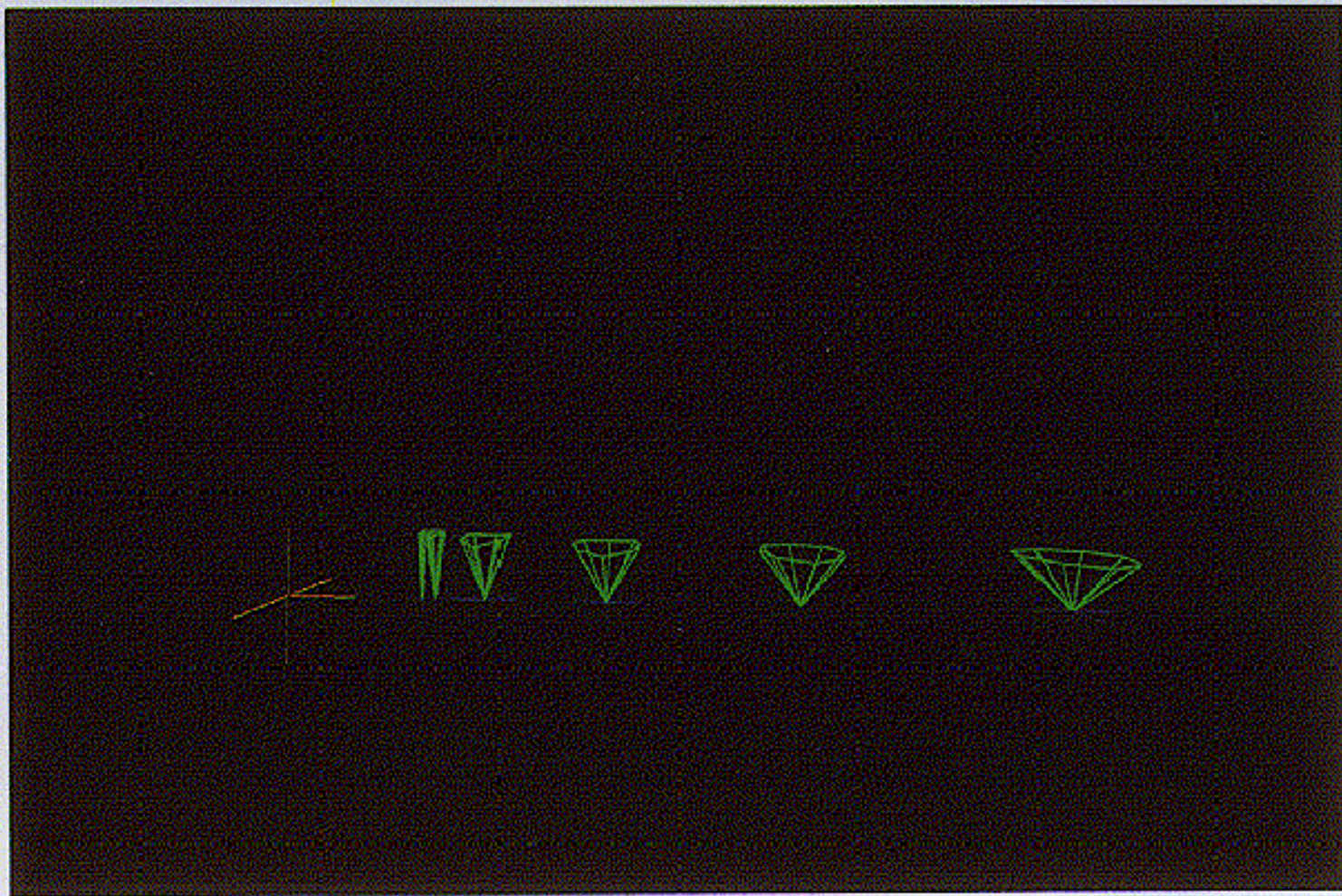


Figure 6: Lightcones.

Spacetime display of light cones at varying distances from the center of the object. Far from the center (right), the lightcone is as wide as it is tall, indicating that the light is travelling out in space as well as forward in time. Near the object the light is moving further in time than in space. At  $r = F(2Gm, c)$  (leftmost case) the light moves only forward in time. This implies that no signal can get from  $r \leq F(2Gm, c)$  to  $r = \text{infinity}$ , so the region  $r < F(2Gm, c)$  is causally disconnected from the rest of the universe.